

Chandra Observations of the Optically Dark GRB 030528

N. Butler*, A. Dullighan*, P. Ford*, G. Ricker*, R. Vanderspek*, K.
Hurley[†], J. Jernigan[†] and D. Lamb**

*Center for Space Research, Massachusetts Institute of Technology, MA

[†]Space Sciences Laboratory, Berkeley, CA

**Department of Astronomy, University of Chicago, IL

Abstract. The X-ray-rich GRB 030528 was detected by the HETE satellite and its localization was rapidly disseminated. However, early optical observations failed to detect a counterpart source. In a 2-epoch ToO observation with Chandra, we discovered a fading X-ray source likely counterpart to GRB 030528. The source brightness was typical of X-ray afterglows observed at similar epochs. Other observers detected an IR source at a location consistent with the X-ray source. The X-ray spectrum is not consistent with a large absorbing column.

OBSERVATIONS

The X-ray-rich (i.e. for the fluence S , $\log[S_X(2 - 30 \text{ keV})/S_\gamma(30 - 400 \text{ keV})] > -0.5$) GRB 030528 was detected by the *HETE* satellite [1] with a $2'$ radius (90% confidence) SXC localization. The initial SXC error region was later revised [17] after the discovery of an unaccounted-for systematic effect, resulting in a shift in position center and an expansion of the error region to $2.5'$ radius. Early R-band observations reaching $R \approx 18.7$ roughly 140 minutes after the burst [2] and unfiltered observations reaching 20.5 magnitude roughly 14 hours after the burst [16] failed to detect a counterpart.

On 3 June, the *Chandra Observatory* targeted the field of GRB 030528 as part of a series of GTO target-of-opportunity observations focusing on optically-dark GRBs discovered by *HETE*. The 25 ksec observation spanned the interval 12:22-20:08 UT, 5.97 - 6.29 days after the burst. The revised SXC error region from Villasenor et al. [17] was completely contained within the field-of-view of the *Chandra* ACIS-S3 chip. From 9 June 8:14 UT to 9 June 14:19 UT, 11.8 to 12.1 days post-burst, *Chandra* again targeted the field of GRB 030528 for a 20 ksec second epoch (E2) observation with ACIS-S3.

CHANDRA E1 SOURCES

As reported in Butler et al. [4], 4 candidate sources were detected within the revised SXC error region. Seven additional non-stellar point sources were detected within the entire ACIS-S3 field-of-view. Positions and other data for these sources are shown in Table 1. None of the sources were anomalously bright relative to objects in *Chandra* deep field observations [see, e.g., 15]. We had performed deep observations with Magellan

prior to the *Chandra* observation, but none of the *Chandra* sources were in our field of view. However, near-IR observations of a portion of the SXC error region containing two of the E1 *Chandra* sources revealed a fading Ks-band source [10]. Between 0.7 and 3.6 days after the burst a fade by 0.9 magnitudes was observed for a source spatially coincident with the brightest *Chandra* source. After the E1 *Chandra* observation, deep observations in the radio (6.8 days after the burst) [9] and in I-band (8.7 days after the burst, $I > 21.5$) [13] failed to detect a counterpart source.

TABLE 1. Four point sources are detected in the 0.5-8.0 keV band in the *Chandra* E1 observation lying within the revised SXC error region. Eight additional, non-stellar point sources are detected in the ACIS-S3 field-of-view. From the E1 net counts, we calculate $E2_{90\%}$, the 90% confidence region for the expected net counts in E2, following Kraft et al. [12]. The columns labeled “ ΔC ” and “ P_C ” are explained in Section . Small values of P_C indicate sources likely to have faded between E1 and E2. Source #17 was situated on a chip gap in E2.

#	Chandra Name	Epoch 1		Epoch 2		ΔC	$P_C^{(\%)}$
		Net (Bg)	$E2_{90\%}$	Net (Bg)			
1	CXOU J170400.3-223710	39.5 (1.5)	24.1,41.1	8.5 (2.5)	6.97	0.01	
4	CXOU J170348.4-223826	30.1 (2.9)	16.4,30.2	20.3 (2.7)	0.01	37.7	
9	CXOU J170400.1-223548	10.8 (2.2)	4.1,12.6	5.4 (3.6)	0.17	28.8	
10	CXOU J170354.0-223654	9.2 (2.8)	3.4,12.6	8.3 (2.7)	0.00	44.7	
...							
2	CXOU J170358.7-224237	30.6 (3.4)	14.1,28.0	23.9 (2.1)	0.00	36.1	
3	CXOU J170355.7-223503	23.1 (2.9)	11.8,24.6	15.1 (3.9)	0.03	2.3	
5	CXOU J170342.8-223548	23.7 (4.3)	12.4,26.0	10.7 (6.3)	0.85	9.8	
8	CXOU J170403.9-223543	12.7 (2.3)	5.7,16.0	4.4 (2.6)	0.94	8.9	
14	CXOU J170341.4-223646	6.1 (4.9)	1.1,9.0	9.7 (5.3)	0.00	48.8	
15	CXOU J170411.2-224032	11.0 (4.0)	4.3,14.4	5.5 (3.5)	0.20	24.1	
17	CXOU J170345.8-224133	10.5 (4.5)	1.1,4.0	...			

AFTERGLOW CONFIRMED IN E2

Table 1 shows the number of counts detected in E1, along with the 90% confidence interval for E2 based on the E1 values. The E2 observations were reported in Butler et al. [5]. We have used a circular extraction region for each source, with radius set to 2 times the 95% encircled energy radius r . This varies over the chip and is approximated via $r = 2.05 - 0.55 * d + 0.18 * d^2$ arcsec, with d measured in arcminutes from the center of the ACIS-S3 chip. We use an annular background region ten times larger than the signal region, centered on and surrounding the signal region. The exposure is calculated separately for each source extraction region in each epoch.

GRB X-ray afterglows typically fade in brightness with time as $t^{-1.3}$, with t measured from the GRB [7]. Assuming no spectral evolution, this implies a count-rate fade factor of approximately 2.5 between E1 and E2. We can test whether the data for each source prefers a fade versus a constant count rate by fitting the data for each source first with a single-rate model (Model A), then fitting the data with a model allowing the E2 rate to be lower than the E1 rate (Model B). We do the fits by maximizing the logarithm of

the Poisson likelihood (i.e. the Cash [6] statistic C). We then simulate 10^4 data sets for each source using the count rate determined from Model A, and we count the number of these which yield a larger ΔC than the observed value when fit with Model B. These fractions are expressed as probabilities (P_C) in Table 1.

Of the four sources in the revised SXC error region (#'s 1,4,9,10), source #1 has faded far below the 90% confidence range established in E1. The significance of the fade is approximately 3σ , and we estimate the temporal index (assuming a power-law fade) to be $\alpha = 2.0 \pm 0.8$. This is somewhat steeper than the typical $t^{-1.3}$ fade for X-ray afterglows [7], though it is characteristic of afterglows which have undergone a so-called “jet-break” [8]. None of the other *Chandra* sources were observed to fade at a high level of significance, and source #1 (also a fading IR source as discussed above) is extremely likely to be counterpart to GRB 030528.

COLUMN DENSITY CONSTRAINTS

We reduce the spectral data using the standard CIAO¹ processing tools. We use “contamarf”² to correct for the quantum efficiency degradation due to contamination in the ACIS chips, important for energies below ~ 1 keV. There are not enough source counts for detailed spectral fitting with the *Chandra* data. However, we can use the instrumental response determined in the steps above in combination with the total number of detected source and background counts in the 0.5-8 keV band (Table 1) and the number of source plus background counts detected in the 0.5-0.6 keV band (2 counts) to constrain the model column density. Assuming a power-law spectrum, Figure 1 shows how the two low-energy counts become increasingly improbable as the column density increases. Except for the case of high redshift ($z > 1$), Figure 1 implies a column density $\lesssim 10^{22}$ cm^{-2} . This implies an extinction in R-band of $A \lesssim 3$ mag. At high redshift ($z \sim 3$), the column is likely $\lesssim 10^{23}$ cm^{-2} .

CONCLUSIONS

An X-ray observation ~ 6 days after GRB 030528 detected the afterglow at a flux level (1.4×10^{-14} $\text{erg cm}^{-2} \text{ s}^{-1}$) typical for GRB X-ray afterglows [see, 7] at that epoch. Here we have assumed a typical power-law spectrum with photon index $\Gamma = 1.9$ and the Galactic $N_H = 1.6 \times 10^{21}$ cm^{-2} . A second epoch observations decisively revealed that source #1 had faded, establishing securely that this was the counterpart X-ray afterglow to GRB 030528. The X-ray spectrum appears to imply a fairly low column density, which in turn implies a fairly low amount of reddening in the source frame. Thus, although the detection of a near-IR counterpart with no detection of an optical counterpart for this burst perhaps points toward dust extinction, we find no supporting

¹ <http://cxc.harvard.edu/ciao/>

² http://space.mit.edu/CXC/analysis/ACIS_Contam/script.html

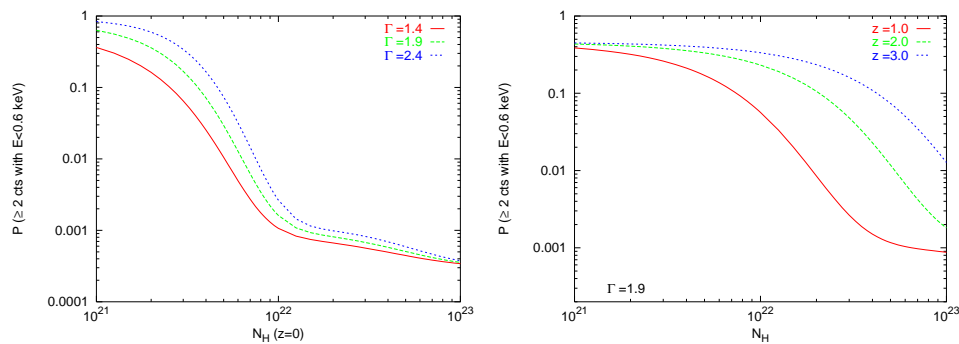


FIGURE 1. The probability is very low that a power-law spectrum with the indices shown (left plot) and $N_H \gtrsim 10^{22} \text{ cm}^{-2}$ could have yielded two source counts below 0.6 keV, as observed. The possibility that the counts could have come from the background is accounted for, using an annular background region approximately 100 times larger than the source region and surrounding the source region. The expected number of background counts in the $3.3''$ radius source extraction region is 0.02 counts. Because the host redshift is unknown, any local contribution in excess of the Galactic column (right plot) may be less well constrained. For $z = 1$, it is likely that the local column is $\lesssim 10^{22} \text{ cm}^{-2}$.

evidence in the X-ray data. The publication of additional photometric data in various passbands for this burst, if available, would help to constrain any possible extinction by dust in the GRB host galaxy. We will perhaps learn that the afterglow to GRB 030528 was intrinsically faint rather than heavily extinguished, as appears to be common in many GRBs [see, e.g., 3, 14].

REFERENCES

1. Atteia, J-L., et al. 2003, *GCN*, 2256
2. Ayani, K., & Yamaoka, H. 2003, *GCN*, 2257
3. Berger, E., et al. 2002, *ApJ*, 581, 981
4. Butler, N. R., et al. 2003a, *GCN*, 2269
5. Butler, N. R., et al. 2003b, *GCN*, 2279
6. Cash, W. 1979, *ApJ*, 228, 939
7. Costa, E., et al. 1999, *A&AS*, 138, 425
8. Frail, D. A., et al. 2001, *ApJ*, 562, L55
9. Frail, D. A., & Berger, E., et al. 2003, *GCN*, 2270
10. Greiner, J., Rau, A., & Klose, S. 2003, *GCN*, 2271
11. Henden, A. 2003, *GCN*, 2267
12. Kraft, R., Burrows, D., & Nousek, J. 1999, *ApJ*, 374, 344
13. Mirabel, N., & Halpern, J. 2003, *GCN*, 2273
14. Ricker, G. R., et al. 2003, *in these proceedings*
15. Rosati, P., et al. 2002, *ApJ*, 566, 667
16. Valentini, G., et al. 2003, *GCN*, 2258
17. Villasenor, J., et al. 2003, *GCN*, 2261